

# A coreless giant vortex in a very strongly dipolar condensate of NaCs molecules

S. K. Adhikari<sup>‡</sup>

Instituto de Física Teórica, UNESP - Universidade Estadual Paulista,  
01.140-070 São Paulo, São Paulo, Brazil

## Abstract.

A strongly dipolar  $^{164}\text{Dy}$  condensate of dipolar length  $a_{\text{dd}} = 130.8a_0$ , with  $a_0$  the Bohr radius, hosts a wide variety of eigenstates, such as droplet, droplet-lattice, and ring-topology states, and self-bound droplets. Motivated by the observation of a very strongly dipolar condensate of NaCs molecules [Bigagli N et al. 2024 Nature 631 289], we demonstrate by numerical simulation, using an improved mean-field model, including the Lee-Huang-Yang interaction, that in a very strongly dipolar NaCs condensate with  $a_{\text{dd}} = 2000a_0$ , most of the above-mentioned states continue to exist and can appear for a much smaller number  $N$  of particles ( $N \gtrsim 1000$ ) within the present experimental possibility. However, in a single-component harmonically-trapped rotating NaCs condensate, a new type of coreless giant-vortex states, with a phase drop of  $2\pi L$  along a closed path around the axis of rotation, appear, where  $L$  is the angular momentum of the vortex.

<sup>‡</sup> sk.adhikari@unesp.br, professores.ift.unesp.br/sk.adhikari/

## 1. Introduction

After the observation of harmonically-trapped Bose-Einstein condensates (BEC) of  $^{87}\text{Rb}$  [1],  $^7\text{Li}$  [2] and  $^{23}\text{Na}$  [3] alkali-metal atoms with magnetic dipole moment  $\mu = \mu_0$ , where  $\mu_0$  is a Bohr magneton, at ultra-low temperatures in a laboratory, there have been many experiments to investigate their properties. Later, it has been possible to create a BEC of  $^{52}\text{Cr}$  [4],  $^{166}\text{Er}$  [5], and  $^{164}\text{Dy}$  [6] atoms [7, 8] with  $\mu = 6\mu_0, 7\mu_0$  and  $10\mu_0$ , respectively, with much stronger dipolar interaction. The dipolar length  $a_{\text{dd}}$ , which is a measure of the strength of dipolar interaction, viz. (2), has the values  $15a_0$ ,  $66a_0$ , and  $130.8a_0$  for  $^{52}\text{Cr}$ ,  $^{166}\text{Er}$ , and  $^{164}\text{Dy}$  atoms [8], respectively, compared to a negligible value for the alkali metal atoms. Because of the strong long-range nonlocal dipolar interaction in these condensates, many new types of states could be realized, which were not possible in the usual alkali-metal-atom condensates dominated by the zero-range contact interaction. In a harmonically trapped  $^{164}\text{Dy}$  condensate, for atomic density above a critical value, the transition to a droplet state, of size much smaller than the typical oscillator trap length, was observed [9, 10] and studied theoretically [11, 12]. In addition, with the increase of the number of atoms, a multiple-droplet supersolid [13, 14] state arranged on a triangular lattice was realized in a quasi two-dimensional (2D) system [9, 15, 16] and theoretically studied [17, 18, 19]. Later, in a strongly dipolar BEC, theoretical studies predicted multiple-droplet states on a square lattice [20], and hollow cylindrical states with a ring topology [21] in harmonically-trapped systems, in addition to self-bound droplets [11, 12] in free space. Quantum states with a distinct topology [22, 23, 24, 25] have been the subject matter of intense investigation in recent times not only in search of new physics but also due to its possible application in quantum information processing [26, 27].

The recent observation of a very strongly dipolar BEC of about 2000 NaCs molecules [28] with a large electric dipole moment, employing the microwave-shielding technique [29, 30, 31], has opened a new avenue of research [32, 33, 34]. Different from an atomic dipolar condensate, the effective electrical dipole moment of a NaCs molecule can be controlled by the microwave-shielding technique [28, 35], which allows to have a NaCs molecular BEC of very large dipolar length  $a_{\text{dd}}$  in the range  $1000a_0$  to  $25000a_0$  [28], compared to  $a_{\text{dd}} = 130.8a_0$  for Dy atoms.

In this paper, we make a comprehensive analysis of the eigenstates of a very strongly dipolar condensate of NaCs molecules polarized along the  $z$  direction. We find that all the above-mentioned states of Dy atoms continue to exist in a molecular NaCs condensate. Moreover, if the relative strength of the dipolar interaction, compared to the contact interaction, is increased, the above-mentioned states of a  $^{164}\text{Dy}$  condensate can be realized in a NaCs condensate for a relatively small number of molecules. In this study, we will consider a dipolar length  $a_{\text{dd}} = 2000a_0$ , achieved by the microwave-shielding technique [28, 35], and a scattering length  $a = 100a_0$ , obtained by the Feshbach-resonance technique [36]. Consequently, for a very strongly dipolar harmonically-trapped NaCs condensate with  $a_{\text{dd}} = 2000a_0$  and  $a = 100a_0$ , a droplet-lattice state with two to nine droplets, as well as a self-bound state, can be formed for a relatively small number of molecules ( $N < 1000$ ), which is within the reach of present experiments, provided that the rapid loss of molecules from the condensate can be controlled experimentally by microwave shielding [28, 35].

In this theoretical investigation we use an improved mean-field model, where we include a Lee-Huang-Yang-type (LHY) interaction [37], appropriate for dipolar molecules [38, 39, 40]. The same model was used recently in the study of the

formation of droplets in a strongly dipolar BEC of dysprosium and erbium atoms [7]. As the dipolar interaction increases beyond a critical value [41], a strongly dipolar BEC collapses in the mean-field Gross-Pitaevskii (GP) model. However, if a LHY interaction [38, 40] is included in the same model, the collapse can be avoided and the dipolar BEC can be stabilized [7]. Once the collapse is excluded, a very strongly dipolar harmonically-trapped condensate of NaCs molecules, with  $a_{\text{dd}} = 2000a_0$  and  $a = 100a_0$ , exhibit different types of eigenstates – the droplet-lattice states for a relatively small number of molecules ( $N \lesssim 1000$ ) in a quasi-two-dimensional (quasi-2D) trap as well as the self-bound droplet states in free space for a very small  $N$ . The droplet-lattice states may have triangular [17] or square [20] symmetry. If a harmonically-trapped very strongly dipolar BEC of NaCS molecules is set to rotation around the dipolar  $z$  axis, a coreless giant-vortex state with a large angular momentum ( $4 \geq L > 1$ ) can be generated for a larger number of molecules ( $N \lesssim 10000$ ). In a nondipolar BEC, a vortex with angular momentum  $L > 1$  is energetically unstable and breaks up into multiple vortices of angular momentum  $L = 1$  each [42, 43, 44, 45, 46, 47]. In view of this, a coreless giant vortex in a strongly dipolar BEC is unexpected. It is the long-range dipolar repulsion in the  $x$ - $y$  plane, which stabilizes the coreless giant vortex. However, if the net dipolar interaction is reduced, by reducing the dipolar length  $a_{\text{dd}}$  of the molecules, the coreless giant-vortex states first become giant-vortex states with a core and with further reduction of  $a_{\text{dd}}$  these states cease to exist.

Previously studied coreless vortex states [48, 49, 50, 51], distinct from the present coreless giant-vortex states, were formed in a nondipolar *multi-component* system, where one of the components did not host a vortex and hence had a non-zero density at the vortex core, while some of the other component(s) had vortices. Consequently, the net total density in such a multi-component coreless vortex state is non-zero at the center of the vortex, although the component density hosting a vortex is zero at the center of the vortex. The present coreless giant-vortex states in a very strongly dipolar rotating single-component molecular NaCs condensate with  $L > 1$  have a non-zero central density.

In section 2 a description of the the mean-field model, with the appropriately modified [38, 40] LHY interaction [37], for a dipolar BEC, with repulsive molecular interaction (positive scattering length), is presented. We also present the same for a rotating dipolar BEC. In section 3 we display numerical results for the formation of different possible states including the droplet-lattice states, self-bound droplet states in a nonrotating BEC of NaCs molecules with a dipolar length  $a_{\text{dd}} = 2000a_0$  and  $a = 100a_0$  as well as the the coreless  $L = 2, 4$  giant vortex states in a rotating BEC of NaCs molecules as obtained by imaginary-time propagation. As the dipolar length  $a_{\text{dd}}$  is reduced to  $1000a_0$ , the  $L = 2$  coreless giant vortex (for  $N = 8000$ ) becomes a usual  $L = 1$  vortex with a core and the  $L = 4$  coreless giant vortex becomes a  $L = 2$  giant vortex with a core. For  $a_{\text{dd}} = 1000a_0$ , we could not find any coreless giant vortex for  $L > 2$ . In section 4 we present a brief summary of our findings.

## 2. Improved mean-field model

The improved GP equation for a very strongly dipolar BEC of  $N$  NaCs molecules polarized along the  $z$  direction, of mass  $m$  each, after the inclusion of the LHY

interaction, can be written as [8, 52, 53, 54]

$$\begin{aligned} i\hbar \frac{\partial \psi(\mathbf{r}, t)}{\partial t} = & \left[ -\frac{\hbar^2}{2m} \nabla^2 + U(\mathbf{r}) + \frac{4\pi\hbar^2}{m} aN |\psi(\mathbf{r}, t)|^2 \right. \\ & + \frac{3\hbar^2}{m} a_{\text{dd}} N \int U_{\text{dd}}(\mathbf{R}) |\psi(\mathbf{r}', t)|^2 d\mathbf{r}' \\ & \left. + \frac{\gamma_{\text{LHY}} \hbar^2}{m} N^{3/2} |\psi(\mathbf{r}, t)|^3 \right] \psi(\mathbf{r}, t), \end{aligned} \quad (1)$$

$$U_{\text{dd}}(\mathbf{R}) = \frac{1 - 3 \cos^2 \theta}{|\mathbf{R}|^3}, \quad a_{\text{dd}} = \frac{m d_{\text{eff}}^2}{12\pi\hbar^2 \epsilon_0}, \quad (2)$$

where the confining axially-symmetric harmonic-oscillator trap  $U(\mathbf{r})$  is given by  $U(\mathbf{r}) = \frac{1}{2}m[\omega_\rho^2(x^2 + y^2) + \omega_z^2 z^2]$ , where  $\omega_\rho$  and  $\omega_z$  are the angular frequencies of the harmonic trap in the  $x$ - $y$  plane and along the  $z$  direction, respectively,  $d_{\text{eff}}$  is the effective electrical dipole moment of a NaCs molecule, controlled by the microwave-shielding technique [28, 35],  $\epsilon_0$  is the permittivity of free space,  $U_{\text{dd}}(\mathbf{R})$  is the anisotropic dipolar interaction between two molecules placed at  $\mathbf{r} \equiv \{\mathbf{x}, \mathbf{y}, \mathbf{z}\}$  and  $\mathbf{r}' \equiv \{\mathbf{x}', \mathbf{y}', \mathbf{z}'\}$  and  $\theta$  is the angle between the vector  $\mathbf{R} \equiv \mathbf{r} - \mathbf{r}'$  and the  $z$  axis, the scattering length  $a$  indicates the strength of the molecular contact interaction, and the dipolar length  $a_{\text{dd}}$ , viz. (2), measures the strength of dipolar interaction; the wave function normalization is  $\int |\psi(\mathbf{r}, t)|^2 d\mathbf{r} = 1$ .

The strength of the LHY interaction [37]  $\gamma_{\text{LHY}}$  in (1), for dipolar molecules [38, 40], is given by [39]

$$\gamma_{\text{LHY}} = \frac{128}{3} \sqrt{\pi a^5} Q_5(\varepsilon_{\text{dd}}), \quad \varepsilon_{\text{dd}} = \frac{a_{\text{dd}}}{a}, \quad (3)$$

where the auxiliary function  $Q_5(\varepsilon_{\text{dd}}) = \int_0^1 dx (1 - \varepsilon_{\text{dd}} + 3x^2 \varepsilon_{\text{dd}})^{5/2}$  can be approximated as [52]

$$\begin{aligned} Q_5(\varepsilon_{\text{dd}}) = & \frac{(3\varepsilon_{\text{dd}})^{5/2}}{48} \Re \left[ (8 + 26\eta + 33\eta^2) \sqrt{1 + \eta} \right. \\ & \left. + 15\eta^3 \ln \left( \frac{1 + \sqrt{1 + \eta}}{\sqrt{\eta}} \right) \right], \quad \eta = \frac{1 - \varepsilon_{\text{dd}}}{3\varepsilon_{\text{dd}}}, \end{aligned} \quad (4)$$

where  $\Re$  is the real part. We will use the analytic approximation (4) for  $Q_5(\varepsilon_{\text{dd}})$  in this study.

The Hamiltonian of a rotating dipolar BEC in the rotating frame is given by [55]

$$H = H_0 - \Omega L_z, \quad (5)$$

where  $H_0$  is the Hamiltonian in the inertial frame and  $L_z \equiv i\hbar(y\partial/\partial x - x\partial/\partial y)$  is the  $z$  component of angular momentum and  $\Omega$  the angular frequency of rotation. Using this transformation, the mean-field GP equation (1) for the trapped BEC in the rotating frame can be written as

$$\begin{aligned} i\hbar \frac{\partial \psi(\mathbf{r}, t)}{\partial t} = & \left[ -\frac{\hbar^2}{2m} \nabla^2 + U(\mathbf{r}) + \frac{4\pi\hbar^2}{m} aN |\psi(\mathbf{r}, t)|^2 \right. \\ & + \frac{3\hbar^2}{m} a_{\text{dd}} N \int U_{\text{dd}}(\mathbf{R}) |\psi(\mathbf{r}', t)|^2 d\mathbf{r}' \\ & \left. + \frac{\gamma_{\text{LHY}} \hbar^2}{m} N^{3/2} |\psi(\mathbf{r}, t)|^3 - \Omega L_z \right] \psi(\mathbf{r}, t). \end{aligned} \quad (6)$$

For  $\Omega > \omega_\rho$ , a harmonically-trapped rotating BEC makes a quantum phase transition to a non-superfluid state, where a mean-field description of the rotating BEC breaks down [56]. In this study we will be confined to the safe domain of ordered rotation of a superfluid with a small velocity:  $\Omega \lesssim 0.6 \times \omega_\rho$ .

To write (6) in the following dimensionless form we express lengths in units of the scale  $l_0 = \sqrt{\hbar/m\omega_z}$ , time in units of  $t_0 = \omega_z^{-1}$ , angular frequency in units of  $\omega_z$ , energy in units of  $\hbar\omega_z$  and density  $|\psi|^2$  in units of  $l_0^{-3}$

$$i\frac{\partial\psi(\mathbf{r}, t)}{\partial t} = \left[ -\frac{1}{2}\nabla^2 + \frac{1}{2}\{\omega_\rho^2(x^2 + y^2) + z^2\} \right. \\ \left. + 4\pi aN|\psi(\mathbf{r}, t)|^2 + 3a_{\text{dd}}N \int U_{\text{dd}}(\mathbf{R})|\psi(\mathbf{r}', t)|^2 d\mathbf{r}' \right. \\ \left. + \gamma_{\text{LHY}}N^{3/2}|\psi(\mathbf{r}, t)|^3 - \Omega L_z \right] \psi(\mathbf{r}, t). \quad (7)$$

Here and in the following, we are representing both the dimensional and the dimensionless variables by the same symbols.

Equation (7) can be obtained from the variational principle  $i\partial\psi/\partial t = \delta E/\delta\psi^*$ , using which we obtain the following expression for the energy functional representing the energy per molecule of a stationary state

$$E = \frac{1}{2} \int d\mathbf{r} \left[ |\nabla\psi(\mathbf{r})|^2 + \{\omega_\rho^2(x^2 + y^2) + z^2\} |\psi(\mathbf{r})|^2 \right. \\ \left. + 3a_{\text{dd}}N|\psi(\mathbf{r})|^2 \int U_{\text{dd}}(\mathbf{R})|\psi(\mathbf{r}')|^2 d\mathbf{r}' + 4\pi Na|\psi(\mathbf{r})|^4 \right. \\ \left. + \frac{4\gamma_{\text{LHY}}}{5}N^{3/2}|\psi(\mathbf{r})|^5 - \Omega\psi^*(\mathbf{r})L_z\psi(\mathbf{r}) \right]. \quad (8)$$

### 3. Numerical Results

The partial differential GP equation (7) is solved numerically by the split-time-step Crank-Nicolson method [57], using the available C or FORTRAN programs [53, 58, 59, 60]. To find a stationary state we used the imaginary-time propagation method. The space steps used for the solution of (7) are  $dx = dy = 0.1$  and  $dz = 0.15$ , and the corresponding time step in imaginary-time propagation is  $dt = 0.1 \times (dxdydz)^{2/3}$ .

The dipolar length and the scattering length of NaCs molecules could be controlled by the microwave shielding [28] and Feshbach resonance [36] techniques, respectively. In this paper, we consider a very strongly dipolar condensate of NaCs molecules with  $a_{\text{dd}} = 2000a_0$  and  $a = 100a_0$ . For NaCs molecules  $m(\text{NaCs}) \approx 156 \times 1.66054 \times 10^{-27}$  kg. Consequently, for  $\omega_z = 2\pi \times 162$  Hz, used in this study as in the pioneering experiment with a NaCs condensate [28], the unit of length is  $l_0 = \sqrt{\hbar/m\omega_z} = 0.6324 \mu\text{m}$ . In this paper, we concentrate on the droplet-lattice states in a harmonically-trapped NaCs BEC, self-bound droplets in a NaCs BEC in free space, and the coreless giant vortices in a rotating harmonically-trapped NaCs BEC. We do not look for and study other types of states, such as [61, 62, 63] the honeycomb and labyrinthine states, as well as a pumpkin-phase state, or a striped supersolid state naturally expected in a strongly dipolar BEC. We will only consider the states with some spatial symmetry. The results of the condensate densities in a three-dimensional (3D) system is often best illustrated by a contour plot of the

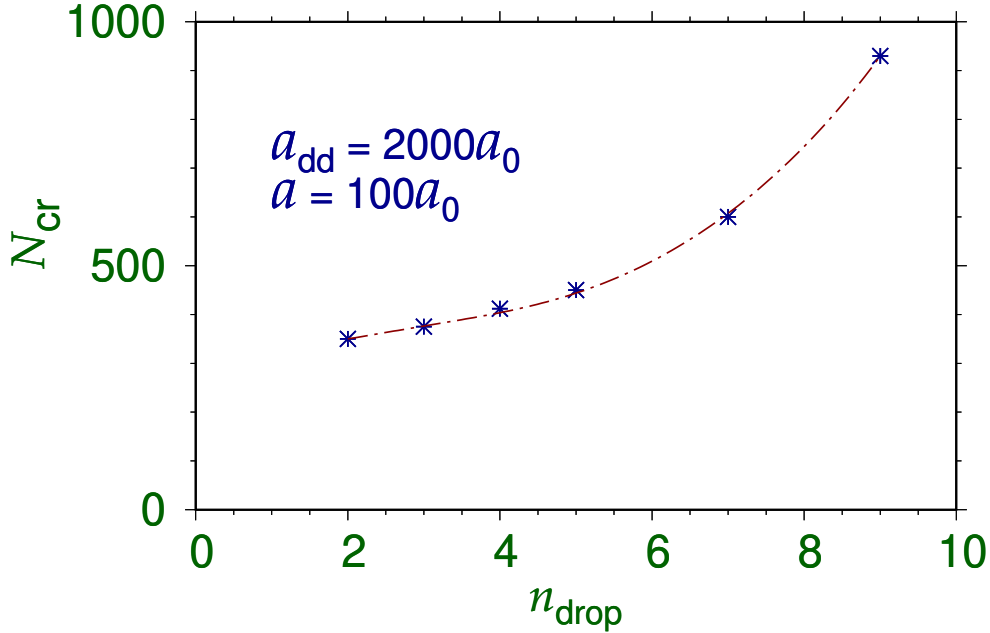


**Figure 1.** Critical number of NaCs molecules  $N_{\text{cr}}$  for the formation of  $n_{\text{drop}}$  ( $=2,3,4,5,7,9$ ) droplets. The parameters of the model are  $a = 100a_0$ ,  $a_{\text{dd}} = 2000a_0$ ,  $\omega_z = 2\pi \times 162$  Hz,  $\omega_\rho = 0.2\omega_z$  in figures 1–3.

integrated 2D density  $n_{2D}(x, y)$  defined by

$$n_{2D}(x, y) = \int_{-\infty}^{\infty} dz |\psi(x, y, z)|^2. \quad (9)$$

Similarly, it is useful to define the following integrated one-dimensional (1D) densities  $n_{1D}(x)$  and  $n_{1D}(z)$  defined by

$$n_{1D}(x) = \int_{-\infty}^{\infty} dz \int_{-\infty}^{\infty} dy |\psi(x, y, z)|^2, \quad (10)$$

$$n_{1D}(z) = \int_{-\infty}^{\infty} dx \int_{-\infty}^{\infty} dy |\psi(x, y, z)|^2. \quad (11)$$

### 3.1. Droplet-lattice state

The lattice symmetry of these states appears in the  $x$ - $y$  plane, perpendicular to the polarization  $z$  direction. For an efficient and quick convergence of a droplet-lattice state in an imaginary-time calculation, an appropriate choice of the initial state is essential. The numerical simulation for a droplet-lattice state was started by many Gaussian droplets arranged on a desired lattice in the  $x$ - $y$  plane [20]. Each droplet has a small extension in the  $x$ - $y$  plane and a relatively larger extension along the  $z$  direction. We investigate a triangular- and square-lattice arrangement of two, three, four, five, seven and nine droplets. The harmonic trap for the study of the droplet-lattice states is a quasi-2D one [17, 18, 19], as in the experiment of NaCs BEC [28], and

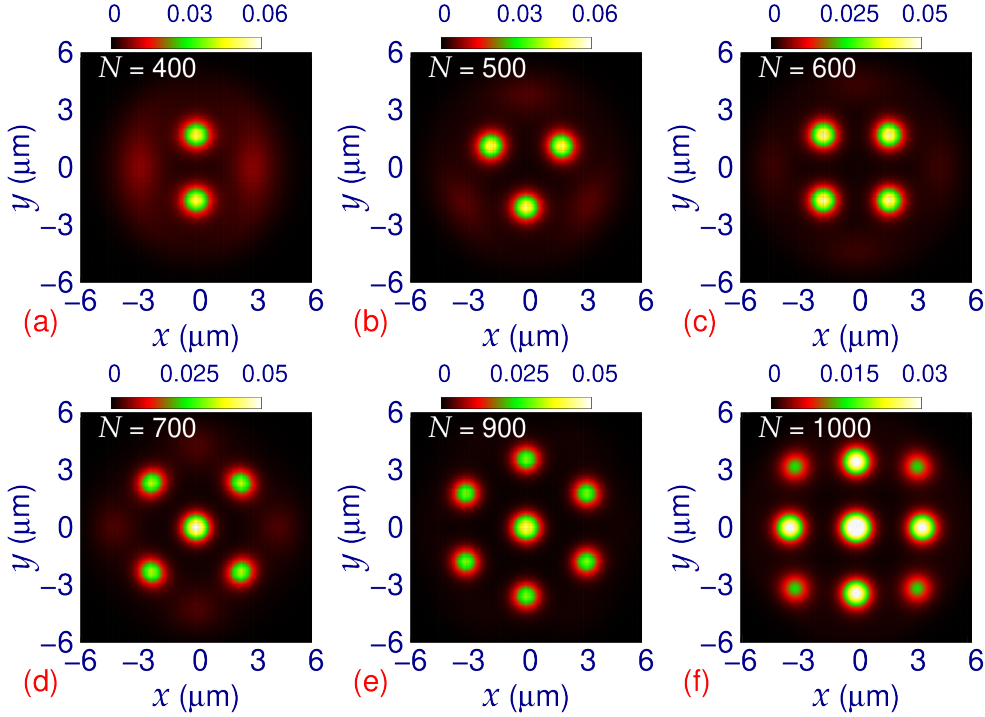


**Figure 2.** Contour plot of dimensionless quasi-2D density  $n_{2D}(x, y)$  of a (a) two-, (b) three-, (c) four-, (d) five-, (e) seven-, and (f) nine-droplet states for different number  $N$  of NaCs molecules.

has the axial and radial angular frequencies  $\omega_z = 2\pi \times 162$  Hz and  $\omega_\rho = 0.2\omega_z \approx 2\pi \times 32$  Hz, respectively.

In a strongly dipolar atomic condensate [9, 10, 15], there is a critical number of atoms for the formation of a certain number  $n_{\text{drop}}$  of droplets. Similarly, in a very strongly dipolar condensate of NaCs molecules, there is a critical number of molecules  $N_{\text{cr}}$  for the creation of a droplet-lattice state of a certain number of droplets. In figure 1 we plot the critical number for the formation of 2, 3, 4, 5, 7, and 9 droplets versus the number  $n_{\text{drop}}$  of droplets. Although,  $N_{\text{cr}}$  increases monotonically with  $n_{\text{drop}}$ , this dependency is nonlinear for a small number of droplets. This dependency is expected to be quasi linear [9, 15] for a larger number of droplets.

In figure 2 we illustrate a (a) two-, (b) three-, (c) four-, (d) five-, (e) seven-, and (f) nine-droplet state through a contour plot of integrated 2D density  $n_{2D}(x, y)$  given by (9) for different numbers  $N = 400, 500, 600, 700, 900, 1000$  of very strongly dipolar NaCs molecules, respectively. The interesting feature of the plots of figure 2 is that these two- to nine-droplet states can be formed for the number of molecules  $N \leq 1000$ . The critical number  $N_{\text{cr}}$  of molecules for the formation of these droplets is even smaller. These numbers for a strongly dipolar  $^{164}\text{Dy}$  condensate are larger by more than an order of magnitude [9, 20] compared to the same for a very strongly dipolar NaCs condensate of this study.

We have seen in figure 1 that there is a critical minimum number of molecules  $N_{\text{cr}}$  for the formation of a droplet-lattice state for a certain number of droplets  $n_{\text{drop}}$ .

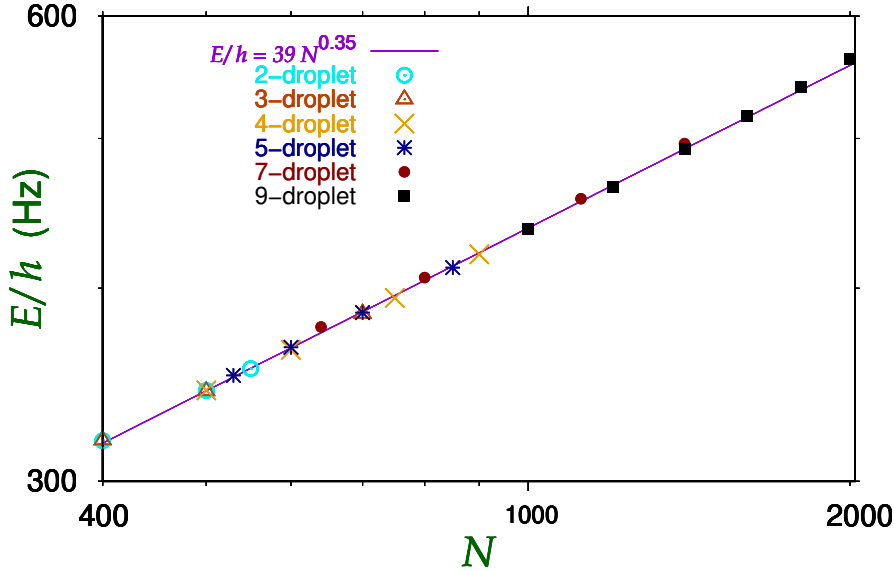


**Figure 3.** The energy per molecule  $E/h$  of droplet-lattice states of three, four, five, six, seven, and nine droplets versus the number  $N$  of NaCs molecules on a log-log scale together with the analytic fit  $E/h = 39N^{0.35}$  (Hz).

There is also a maximum number of molecules for the formation of a droplet-lattice state for a certain number of droplets  $n_{\text{drop}}$ . In fact, there is a window of  $N$  values for the formation of a state with a certain number of droplets. If  $N$  is larger, more droplets are formed spontaneously. We obtained numerically the energy of these droplet-lattice states for different  $N$ , as obtained from (8), and illustrate these energies  $E/h$  versus  $N$  in figure 3. In Ref. [20] we found that such energies for a strongly dipolar  $^{164}\text{Dy}$  BEC as a function of the number  $N$  of atoms for different droplet-lattice states satisfy a universal scaling  $E \sim N^{0.4}$ . From figure 3 we find a similar scaling  $E \sim N^{0.35}$  in a very strongly dipolar NaCs molecular BEC. It is gratifying to notice that the two exponents of these scalings in a strongly dipolar  $^{164}\text{Dy}$  BEC and in a very strongly dipolar NaCs molecular BEC are quite similar, which confirms the universal nature of the formation of the droplet-lattice states in both systems.

The energies of the triangular and square droplet-lattice states are practically the same for the same number of molecules  $N$ . The same was true in the case of a strongly dipolar  $^{164}\text{Dy}$  condensate [20]. In Ref. [64], we demonstrated in extensive studies of dynamics that both triangular and square droplet-lattice states are dynamically stable and can execute dipole-mode and scissors-mode oscillation for a long time. The distinct symmetry property of these states hinders the easy passage from one type of state to the other.

### 3.2. Self-bound droplet in free space

Self-bound droplets in free space, in the form of an elongated solid cylinder, have been studied in a strongly dipolar condensate of  $^{164}\text{Dy}$  atoms [15, 11, 12]. To find a self-bound droplet in a very strongly dipolar condensate of NaCs molecules by imaginary-



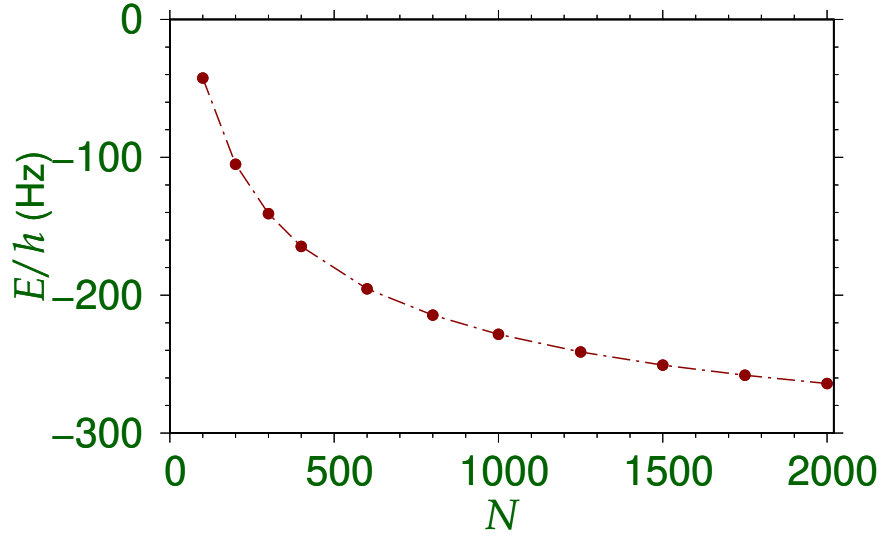


**Figure 4.** The energy per molecule  $E/h$  of self-bound droplets of different number  $N$  of NaCs molecules in free space. The parameters of the model are  $a = 100a_0$ ,  $a_{\text{dd}} = 2000a_0$  in figures 4- 6.

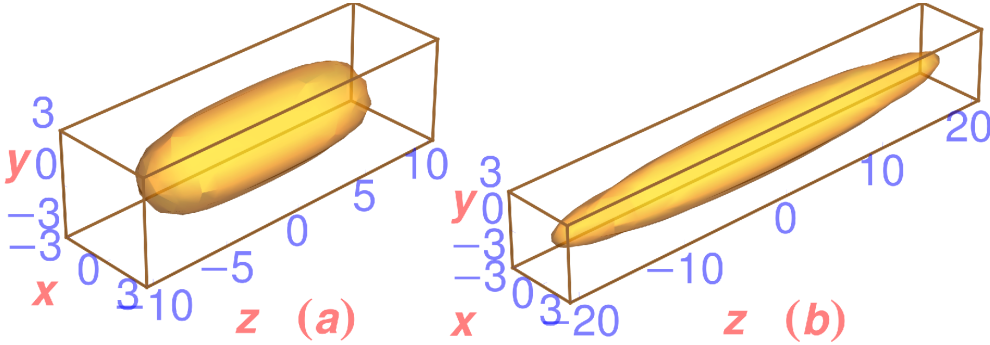


**Figure 5.** Isodensity contour of normalized 3D density  $|\psi(x, y, z)|^2$  of a self-bound droplet of (a)  $N = 100$  and (b)  $N = 1000$  NaCs molecules. The density on the contour is  $10^9$  molecules /  $\text{cm}^3$ . The unit of length  $l_0 = 0.6324 \mu\text{m}$ .

time propagation, we remove the harmonic oscillator trap in (7) and solve it with the following initial wave function in the form of an elongated cylinder:

$$\psi(\mathbf{r}) = \frac{\pi^{-3/4}}{\sqrt{\delta_z \delta_\perp}} \exp \left[ -\frac{x^2 + y^2}{2\delta_\perp^2} - \frac{z^2}{2\delta_z^2} \right], \quad (12)$$

where  $\delta_z$  and  $\delta_\perp$  ( $\delta_z \gg \delta_\perp$ ) are the widths of the Gaussian wave function. It was possible to have a self-bound droplet for different number of molecules  $N$ . In this case the energy is always negative and decreases as the number of molecules increases. In figure 4 we display a plot of energy per molecule  $E/h$  in Hz of a self-bound droplet, as obtained from (8), versus the number of molecules. For a large number of molecules, the energy per molecule saturates with a lower bound for large  $N$ . Hence, for very

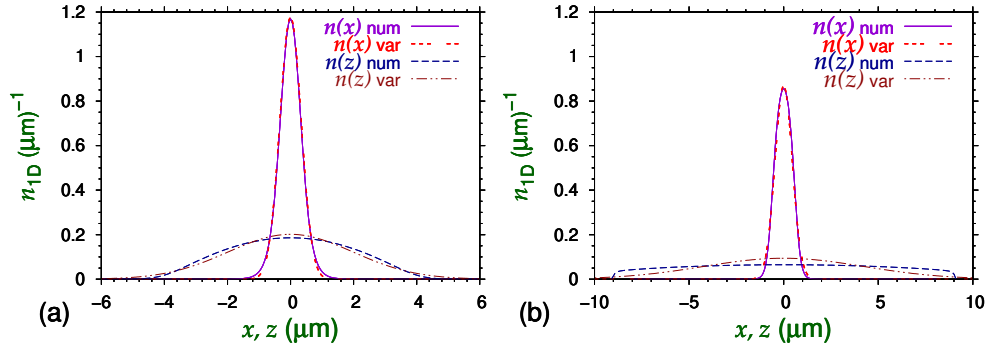


**Figure 6.** Numerical (num) and variational (var) reduced 1D densities  $n_{1D}(x)$  and  $n_{1D}(z)$  along  $x$  and  $z$  directions, respectively, of the two self-bound droplets of figure 5 for (a)  $N = 100$  and (b)  $N = 1000$  NaCs molecules.

large  $N$ , the total energy of a droplet will be linearly proportional to the total number of molecules in the droplet. This behavior of energy is quite different from that of a trapped system, as shown in figure 3, where the energy per molecule always increases with the number of molecules.

These self-bound droplets in a very strongly dipolar NaCs molecular BEC has a very compact shape as can be found from the 3D isodensity plot of  $|\psi(x, y, z)|^2$  of the present droplets in figure 5 of (a)  $N = 100$  and (b)  $N = 1000$  molecules. The droplets are elongated along the polarization  $z$  direction due to the dipolar attraction. Consequently, the self-bound droplet in figure 5(b) for  $N = 1000$  is longer than that the same in figure 5(a) for  $N = 100$ , due to a larger dipolar interaction in the former. In figure 6 we plot the integrated 1D densities  $n_{1D}(x)$  and  $n_{1D}(z)$  given by (10) and (11), respectively, of the two self-bound droplets presented in figures 5(a)-(b) and compare these densities with the variational approximations for the same. The formulation of the variational approximation using the axially-symmetric Gaussian ansatz (12) for the stationary wave function of the self-bound droplet is given in detail in Refs. [53, 65]. The agreement between the numerical result and the variational approximation of the integrated 1D densities of the two self-bound droplets is quite satisfactory, although there is some discrepancy between the variational and numerical results of  $n_{1D}(z)$ , especially for  $N = 1000$ . In that case the numerical density is quite different from a simple Gaussian behavior. The length of the droplet of  $N = 100$  molecules is about  $10 \mu\text{m}$  and that of  $N = 1000$  molecules is about  $20 \mu\text{m}$ .

### 3.3. Coreless giant vortex

To facilitate the numerical simulation of a coreless giant vortex by imaginary-time propagation we use the following phase-imprinted Gaussian initial state, as in Ref. [66],

$$\psi(\mathbf{r}) \sim (x + iy)^L \exp \left[ -\frac{x^2 + y^2}{2\delta_{\perp}^2} - \frac{z^2}{2\delta_z^2} \right]. \quad (13)$$

where  $L$  is the angular momentum of the vortex. The prefactor  $(x + iy)^L$  prints the correct phase on the condensate wave function. To find a coreless giant vortex with a fixed angular momentum  $L$ , the angular frequency of rotation is gradually increased

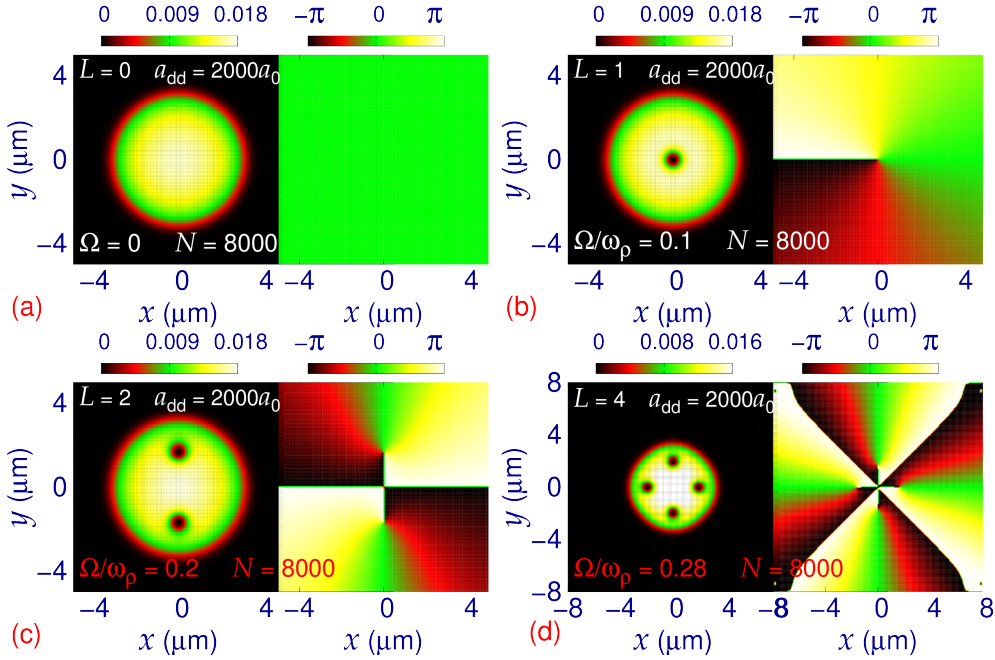


**Figure 7.** Contour plot of dimensionless integrated 2D density (left panel)  $n_{2D}(x, y)$  of the (a) nonrotating ( $L = 0, \Omega = 0$ ) and the (b) rotating vortex ( $L = 1, \Omega/\omega_p = 0.1$ ) state and the corresponding phase of the wave function  $\psi(x, y, 0)$  (right panel). The same of the coreless giant-vortex states for (c)  $L = 2, \Omega/\omega_p = 0.2$  and (d)  $L = 4, \Omega/\omega_p = 0.28$ . The parameters of the model are  $a = 100a_0$ ,  $a_{dd} = 2000a_0$ ,  $\omega_z = 2\pi \times 162$  Hz,  $\omega_p = 0.75\omega_z$ , and  $N = 8000$ .

in imaginary-time propagation till the giant vortex can be obtained. The angular momentum of the obtained giant vortex is confirmed from a contour plot of the phase of the wave function  $\psi(x, y, 0)$  in the  $x$ - $y$  plane. The phase jump of  $2\pi L$  around a closed contour containing the  $x = y = 0$  point confirms a giant vortex of angular momentum  $L$ .

After a small experimentation we find that a coreless giant vortex can be obtained only for  $N$  greater than a critical value of a few thousand molecules. Also, the angular frequency of the transverse trap has to be significantly increased to have a giant-vortex state. In the pursuit of a coreless giant vortex we consider  $N = 2000$  to  $8000$  and  $\omega_p = 0.75\omega_z \approx 2\pi \times 122$  Hz, maintaining  $\omega_z = 2\pi \times 162$  Hz,  $a = 100a_0$  and  $a_{dd} = 2000a_0$ . A coreless giant vortex of angular momentum  $L = 2$  to  $4$  as well as a normal vortex of angular momentum  $L = 1$  is obtained by imaginary-time propagation using the initial function (13). However, for a larger  $L$  ( $> 4$ ) a coreless giant vortex could not be stabilized and it breaks into multiple vortices of smaller  $L$  each.

The numerically obtained  $L = 0, \Omega = 0$  and  $L = 1, \Omega/\omega_p = 0.1$  states for  $N = 8000$  are axially-symmetric cylindrical states. The  $L = 1$  state is easily stabilized and has a central core of very small radius. This is illustrated through a contour plot of dimensionless integrated 2D density  $n_{2D}(x, y)$  (left panel) and the phase of wave function  $\psi(x, y, 0)$  (right panel) in figures 7 (a)  $L = 0, \Omega = 0$  and (b)  $L = 1, \Omega/\omega_p = 0.1$ . An imaginary-time calculation with the initial state (13) for

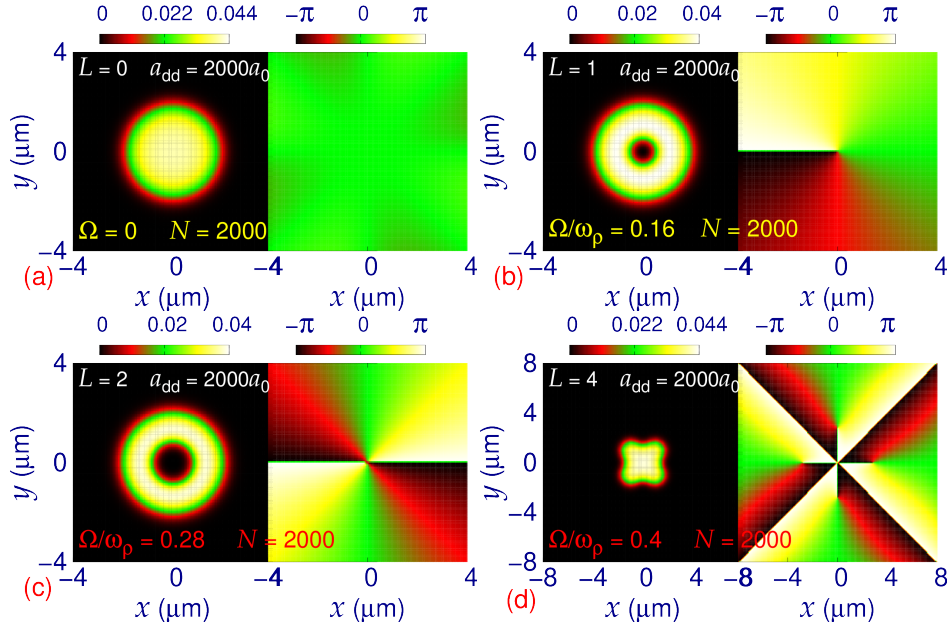


**Figure 8.** The same as in figure 7 of the nonrotating (a)  $L = 0, \Omega = 0$  state, the vortex for (b)  $L = 1, \Omega/\omega_\rho = 0.16$ , the coreless giant vortices for (c)  $L = 2, \Omega/\omega_\rho = 0.28$ , and (d)  $L = 4, \Omega/\omega_\rho = 0.4$ . The other parameters of the model are  $N = 2000, a = 100a_0, a_{dd} = 2000a_0, \omega_z = 2\pi \times 162$  Hz,  $\omega_\rho = 0.75\omega_z$ .

$2 \leq L \leq 4$  naturally leads to the desired coreless giant-vortex states. A coreless giant vortex for  $L = 2$  and  $4$  was stabilized for rotational frequencies  $\Omega/\omega_\rho = 0.2$  and  $0.28$ , respectively, as displayed in figures 7(c)-(d) through a contour plot of  $n_{2D}(x, y)$  and the phase of the wave function  $\psi(x, y, 0)$ , respectively. The giant-vortex states for  $L = 2, 4$  have two and four holes resembling vortex cores, but the phase is uniform at these points without any singularity. There is a phase drop of  $2\pi L$  of the wave function  $\psi(x, y, 0)$  along a closed path around the origin, where the density is non zero, indicating a coreless giant vortex of angular momentum  $L > 1$  located at the center of the condensate. Due to the very strong dipolar attraction, the vortex core has disappeared in the coreless giant vortices of angular momentum  $L = 2, 4$  in figures 7(c)-(d).

We next investigate the fate of the coreless giant vortices as the parameters of the model are changed in order to reduce the net dipolar interaction, which can be achieved by either reducing the dipolar length  $a_{dd}$  or the number of molecules  $N$ . First we consider a reduced value of  $N$ . If  $N$  is reduced to  $N = 2000$  maintaining  $a_{dd} = 2000a_0$  and  $a = 100a_0$ , as in figure 7, the coreless giant vortex of  $L = 4$  continues to exist till a much smaller value of  $N$  ( $N \gtrsim 1500$ ). However, the giant vortex of  $L = 2$  develops a core. This is displayed, for  $N = 2000$ , through a contour plot of the density  $n_{2D}(x, y)$  and the phase of the wave function  $\psi(x, y, 0)$  in figure 8 for (a)  $L = 0, \Omega = 0$ , (b)  $L = 1, \Omega/\omega_\rho = 0.16$ , (c)  $L = 2, \Omega/\omega_\rho = 0.28$ , and (d)  $L = 4, \Omega/\omega_\rho = 0.4$ . Again, due to a reduced dipolar and contact interaction we needed a larger angular frequency of rotation in figure 8 to stabilize a specific vortex or giant vortex, when compared to the same in figure 7. In a nondipolar BEC, we had a similar scenario that the number

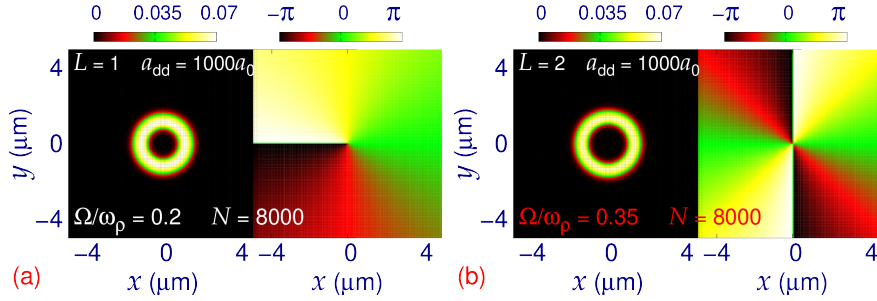


**Figure 9.** The same as in figure 7 of the rotating vortex for (a)  $L = 1, \Omega/\omega_\rho = 0.27$  and the rotating giant vortex for (b)  $L = 2, \Omega/\omega_\rho = 0.35$ . The other parameters of the model are  $N = 8000, a = 100a_0, a_{dd} = 1000a_0, \omega_z = 2\pi \times 162$  Hz,  $\omega_\rho = 0.75\omega_z$ .

of vortices in a BEC can be increased by either increasing the strength of nonlinearity or the angular frequency of rotation [60].

A reduced value of  $a_{dd}$ , which can be achieved by the microwave-shielding technique [28] is considered next. The vortex core may appear as we reduce the strength of the dipolar interaction by considering  $a_{dd} = 1000a_0$  in place of  $a_{dd} = 2000a_0$  in figure 7. The results for the integrated 2D density  $n_{2D}(x, y)$  (left panel) and the phase of the wave function  $\psi(x, y, 0)$  (right panel) as obtained by imaginary-time propagation with the appropriate initial state (13) for  $a_{dd} = 1000a_0$  and  $a = 100a_0$  are displayed in figures 9 for (a)  $L = 1, \Omega/\omega_\rho = 0.2, N = 8000$  and (b)  $L = 2, \Omega/\omega_\rho = 0.35, N = 8000$ . The phase of the vortex states in figures 9(a)-(b) confirms an angular momenta of  $L = 1, 2$ , respectively. In contrast to the  $a_{dd} = 2000a_0$  state displayed in figure 7(d), the state with  $N = 8000, a_{dd} = 1000a_0$  could not be stabilized to produce a  $L = 4$  giant vortex for any  $\Omega$ . The nonlinearities of the states presented in figure 9 are less than the same in figure 7; consequently, a larger angular frequency of rotation is necessary to stabilize the respective vortices in figure 9. The very strong dipolar interaction in the states of figures 7, 8 and 9 is responsible for the generation of the giant vortices. However, due to a reduced net dipolar interaction resulting from a reduced value of  $a_{dd}$ , the states in figure 9(b), when compared to the same in figure 7(c), has developed a vortex core at the center. Consequently, the coreless  $L = 2$  giant vortex has become a giant vortex with a core.

It is interesting to inquire the fate of the giant vortices of figures 7 and 8 as the angular frequency of rotation  $\Omega$  is increased further. We could not find any giant vortex with  $L > 4$  even for a larger  $\Omega$ . This is illustrated in figure 10 (a) for  $\Omega/\omega_\rho = 0.45, N = 8000$  and (b) for  $\Omega/\omega_\rho = 0.6, N = 2000$  representing the giant vortices of figures 7(d) and 8(d), respectively, with an increased frequency of rotation. Nevertheless, four new vortices have appeared in figure 10(a) and eight new vortices in figure 10(b), thus making the total angular momentum  $L = 8$  and 12 in these plots, respectively. In both cases a coreless giant vortex of  $L = 4$  continues to exist at the center. All other vortices in these plots have unit angular momentum.

It has been demonstrated that often a ring-shaped trapped nondipolar [67] and dipolar [68, 69] BECs host a persistent current, which is a vortex-like state showing a phase drop along a closed path including the origin as appropriate for a vortex, even for a zero angular frequency of rotation. Typically, a persistent current was generated

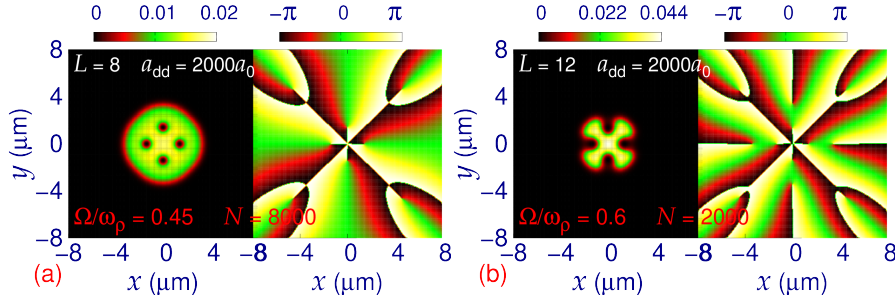


**Figure 10.** The same as in figure 7 of the rotating vortex for (a)  $L = 8, \Omega/\omega_\rho = 0.45, N = 8000$  and for (b)  $L = 12, \Omega/\omega_\rho = 0.6, N = 2000$ . The other parameters of the model are  $a = 100a_0, a_{\text{dd}} = 2000a_0, \omega_z = 2\pi \times 162 \text{ Hz}, \omega_\rho = 0.75\omega_z$ .

by imprinting a vortex on a stable ring-shaped condensate in an appropriate (non-harmonic) trap. We verified that such persistent current is not possible in the present very strongly dipolar NaCs BEC in the absence of rotation and the giant vortices presented in this paper disappear as the angular frequency of rotation is reduced to zero and, hence, are not persistent currents.

#### 4. Summary

We have studied the different possible eigenstates of a very strongly dipolar condensate of NaCs molecules employing an improved GP equation including a repulsive LHY interaction [37] appropriate for dipolar [38, 39, 40] atoms and molecules. Specifically, for dipolar length and scattering length  $a_{\text{dd}} = 2000a_0, a = 100a_0$ , respectively, we investigated the droplet-lattice states in a harmonically-trapped system, self-bound droplets in free space, and novel coreless giant vortices in a rotating harmonically-trapped system. The coreless giant vortices appear for angular momentum  $4 \geq L \geq 2$  and for number of molecules  $N \gtrsim 1500$ . As the dipolar length is reduced, for example to  $a_{\text{dd}} = 1000a_0$ , the  $L = 2$  coreless giant vortex become a normal giant vortex possessing the shape of a hollow cylinder. We could not stabilize a giant vortex with  $L > 2$  and  $a_{\text{dd}} = 1000a_0$ . However, these states are not possible if either  $a_{\text{dd}}$  or  $N$  or both are reduced significantly, so that the dipolar interaction becomes too weak to support a giant vortex.

The presence of electric or microwave fields, in microwave-shielded dipolar BEC, can modify the long-range forces between ultracold dipolar molecules [32, 33, 35, 70] in a way, which is not yet quite understood. These beyond mean-field corrections will be very important for large nonlinearities in (1) for a very large number of molecules, when the gas parameter  $n^{1/3}a$  (or  $n^{1/3}a_{\text{dd}}$ ) becomes comparable to 1, where  $n$  is the density. Most of the results presented in this paper, employs the number of molecules  $N < 2000$  resulting in a negligibly small gas parameter. In this domain the improved mean-field equation (1) is expected to be valid, although it might require some yet unknown correction. In view of this, we do not believe that the qualitative results about the existence of supersolid states, self-bound states, and coreless giant vortices, obtained in this paper, to be so peculiar as to have no general validity.

## Acknowledgments

SKA acknowledges partial support by the CNPq (Brazil) grant 301324/2019-0.

## References

- [1] Anderson M H, Ensher J R, Matthews M R, Wieman C E and Cornell E A 1995 *Science* 269 198
- [2] Bradley C C, Sackett C A and Hulet R G 1997 *Phys. Rev. Lett.* 78 985
- [3] Davis K B, Mewes M-O, Andrews M R, van Druten N J, Durfee D S, Kurn D M and Ketterle W 1995 *Phys. Rev. Lett.* 75 3969
- [4] Lahaye T, Koch T, Fröhlich B, Fattori M, Metz J, Griesmaier A, Giovanazzi S and Pfau T 2007 *Nature* 448 672
- [5] Aikawa K, Frisch A, Mark M, Baier S, Rietzler A, Grimm R and Ferlaino F 2012 *Phys. Rev. Lett.* 108 210401
- [6] Lu M, Youn S H and Lev B L 2010 *Phys. Rev. Lett.* 104 063001
- [7] Chomaz L, Ferrier-Barbut I, Ferlaino F, Laburthe-Tolra B, Lev B L, and Pfau T 2023 *Rep. Prog. Phys.* 86 026401
- [8] Lahaye T, Menotti C, Santos L, Lewenstein M and Pfau T 2009 *Rep. Prog. Phys.* 72 126401
- [9] Kadau H, Schmitt M, Wenzel M, Wink C, Maier T, Ferrier-Barbut I and Pfau T 2016 *Nature* 530 194
- [10] Ferrier-Barbut I, Kadau H, Schmitt M, Wenzel M and Pfau T 2016 *Phys. Rev. Lett.* 116 215301
- [11] Wächtler F and Santos L 2016 *Phys. Rev. A* 94 043618
- [12] Baillie D, Wilson R M, Bisset R N and Blakie P B 2016 *Phys. Rev. A* 94 021602
- [13] Boninsegni M and Prokof'ev N V 2012 *Rev. Mod. Phys.* 84 759
- [14] Yukalov V I 2020 *Physics* 2 49
- [15] Schmitt M, Wenzel M, Böttcher F, Ferrier-Barbut I and Pfau T 2016 *Nature* 539 259
- [16] Norcia M A, Politi C, Klaus L, Poli E, Sohmen M, Mark M J, Bisset R, Santos L and Ferlaino F 2021 *Nature* 596 357
- [17] Poli E, Bland T, Politi C, Klaus L, Norcia M A, Ferlaino F, Bisset R N and Santos L 2021 *Phys. Rev. A* 104 063307
- [18] Baillie D and Blakie P B 2018 *Phys. Rev. Lett.* 121 195301
- [19] Zhang Y-C, Pohl T and Maucher F 2021 *Phys. Rev. A* 104 013310
- [20] Young-S L E. and Adhikari S K 2022 *Phys. Rev. A* 105 033311
- [21] Young-S L E. and Adhikari S K 2023 *Phys. Rev. A* 108 053323
- [22] Hasan M Z and Kane C L 2010 *Rev. Mod. Phys.* 82 3045
- [23] Qi X-L and Zhang S-C 2011 *Rev. Mod. Phys.* 83 1057
- [24] Chiu C-K, Teo Y C Y, Schnyder A P and Ryu S 2016 *Rev. Mod. Phys.* 88 035005
- [25] Móller N S, dos Santos F E A, Bagnato V S and Pelster A 2020 *New J. Phys.* 22 063059
- [26] Stern A and Lindner N H 2013 *Science* 339 1179
- [27] Cornish S L, Tarbutt M R and Hazzard K R A 2024 *Nature Phys.* 20 730
- [28] Bigagli N, Yuan W, Zhang S, Bulatovic B, Karman T, Stevenson I and Will S 2024 *Nature* 631 289
- [29] Anderegg L, Burchesky S, Bao Y, Yu S S, Karman T, Chae E, Ni K K, Ketterle W and Doyle J M 2021 *Science* 373 779
- [30] Schindewolf A, Bause R, Chen X-Y, Duda M, Karman T, Bloch I and Luo X-Y 2022 *Nature* 607 677
- [31] Lin J, Chen G, Jin M, Shi Z, Deng F, Zhang W, Quémener G, Shi T, Yi S and Wang D 2023 *Phys. Rev. X* 13 031032
- [32] Xu B, Yang F, Qi R, Zhai H and Zhang P 2024 [arXiv:2410.10806](https://arxiv.org/abs/2410.10806)
- [33] Langen T, Boronat J, Sánchez-Baena J, Bombín R, Karman T and Mazzanti F 2024 [arXiv:2407.09391](https://arxiv.org/abs/2407.09391)
- [34] Li H, Yu X-H, Nakagawa M and Ueda M 2024 [arXiv:2406.08868](https://arxiv.org/abs/2406.08868)
- [35] Quémener G, Bohn J L and Croft J F E 2023 *Phys. Rev. Lett.* 131 043402
- [36] Chin C, Grimm R, Julienne P S and Tiesinga E 2010 *Rev. Mod. Phys.* 82 1225
- [37] Lee T D, Huang K and Yang C N 1957 *Phys. Rev.* 106 1135
- [38] Lima A R P and Pelster A 2011 *Phys. Rev. A* 84 041604(R)
- [39] Lima A R P and Pelster A 2012 *Phys. Rev. A* 86 063609
- [40] Schützhold R, Uhlmann M, Xu Y and Fischer U R 2006 *Int. J. Mod. Phys. B* 20 3555
- [41] Koch T, Lahaye T, Metz J, Fröhlich B, Griesmaier A and Pfau T 2008 *Nature Phys.* 4 218

- [42] Lundh E 2002 Phys. Rev. A 65 043604
- [43] Kasamatsu K, Tsubota M, and Ueda M 2002 Phys. Rev. A 66 053606
- [44] Fischer U R and Baym G 2003 Phys. Rev. Lett. 90 140402
- [45] Aftalion A and Danaila I 2004 Phys. Rev. A 69 033608
- [46] Fetter A L 2001 Phys. Rev. A 64 063608
- [47] Simula T P, Virtanen S M M and Salomaa M M 2002 Phys. Rev. A 65 033614
- [48] Mermin N D and Ho T-L 1976 Phys. Rev. Lett. 36 594
- [49] Anderson P W and Toulouse G 1977 Phys. Rev. Lett. 38 508
- [50] Mizushima T, Machida K and Kita T 2002 Phys. Rev. Lett. 89 030401
- [51] Mizushima T, Machida K and Kita T 2002 Phys. Rev. A 66 053610
- [52] Bisset R N, Wilson R M, Baillie D and Blakie P B 2016 Phys. Rev. A 94 033619
- [53] Kishor Kumar R, Young-S. L E, Vudragović D, Balaž A, Muruganandam P and Adhikari S K 2015 Comput. Phys. Commun. 195 117
- [54] Yukalov V I 2018 Laser Phys. 28 053001
- [55] Landau L D and Lifshitz E M 1960 “Mechanics”, Pergamon Press, Oxford, Section 39.
- [56] Fetter A L 2009 Rev. Mod. Phys. 81, 647 (2009).
- [57] Muruganandam P and Adhikari S K 2009 Comput. Phys. Commun. 180 1888
- [58] Young-S. L E, Muruganandam P, Balaž A and Adhikari S K 2023 Comput. Phys. Commun. 286 108669
- [59] Lončar V, Young-S. L E, Škrbić S, Muruganandam P, Adhikari S K and Balaž A 2016 Comput. Phys. Commun. 209 190
- [60] Kishor Kumar R, Lončar V, Muruganandam P, Adhikari S K and Balaž A 2019 Comput. Phys. Commun. 240 74
- [61] Hertkorn J, Schmidt J-N, Guo M, Böttcher F, Ng K S H, Graham S D, Uerlings P, Langen T, Zwierlein M and Pfau T 2021 Phys. Rev. Res. 3 033125
- [62] Zhang Y-C, Pohl T and Maucher F 2024 Phys. Rev. Research 6 023023
- [63] Zhang Y-C, Pohl T and Maucher F 2021 Phys. Rev. A 104 013310
- [64] Young-S L E. and Adhikari S K 2023 Phys. Rev. A 107 053318
- [65] Young-S. L E and Adhikari S K 2022 Commun. Nonlin. Sci. Numer. Simul. 115 106792
- [66] Leanhardt A E, Görlitz A, Chikkatur A P, Kielpinski D, Shin Y, Pritchard D E and Ketterle W 2002 Phys. Rev. Lett. 89 190403
- [67] Ryu C, Andersen M F, Cladé P, Natarajan V, Helmerson K and Phillips W D 2007 Phys. Rev. Lett. 99 260401
- [68] Malet F, Kavoulakis G M and Reimann S M 2011 Phys. Rev. A 84 043626
- [69] Nilsson Tengstrand M, Boholm D, Sachdeva R, Bengtsson J and Reimann S M 2021 Phys. Rev. A 103 013313
- [70] Deng F, Chen X-Y, Luo X-Y, Zhang W, Yi S and Shi T 2023 Phys. Rev. Lett. 130 183001